Organometallics **1998,** *17,* 4477−4483 4477

Synthesis, Structure, and Electrochemical Studies of μ_3-η^2,η^2,η^2-C_{60} Triosmium Complexes

Hyunjoon Song,[†] Kwangyeol Lee,[†] Joon T. Park,*[,†] and Moon-Gun Choi[‡]

Department of Chemistry, Korea Advanced Institute of Science and Technology,
Taejon 305-701, Korea, and Department of Chemistry, Yonsei University,
Seoul, 120-749, Korea

Received May 11, 1998

Two μ_3-η^2,η^2,η^2-C_{60} complexes, $Os_3(CO)_8(PPh_3)(\mu_3$-η^2,η^2,η^2-$C_{60})$ (**8**) and $Os_3(CO)_7(PMe_3)_2(\mu_3$-$\eta^2,\eta^2,\eta^2$-$C_{60})$ (**9**), have been prepared by decarbonylation of $Os_3(CO)_9(\mu_3$-η^2,η^2,η^2-$C_{60})$ (**6**) with Me_3NO/MeCN in the presence of phosphine ligands. The molecular structure of **8** has been determined by a single-crystal X-ray diffraction study. The structure of **8** is derived from that of $Os_3(CO)_{11}(PPh_3)$ by replacing three axial carbonyl ligands with a μ_3-face-capping C_6 ring of C_{60}. The ^{13}C NMR spectra (C_{60} region) of **6** and $Os_3(CO)_8(PMe_3)(\mu_3$-η^2,η^2,η^2-$C_{60})$ (**7**) show 11 sp^2 and 1 sp^3 carbon resonances and 29 sp^2 and 3 sp^3 carbon resonances, respectively, which are consistent with C_{3v} and C_s symmetric nature of the two complexes in solution. Electrochemical properties of **6**, **7**, and **9** have been studied by cyclic voltammetry (CV) in 1,2-dichlorobenzene (DCB) solutions. The general features of CV curves have revealed four reversible redox couples for **6** and **7** and three for **9** in the DCB potential window. The μ_3-η^2,η^2,η^2-C_{60} complexes, **6**, **7**, and **9**, show a remarkable electrochemical stability compared to the known η^2-C_{60} triosmium carbonyl complexes. The CV results suggest that a C_{60}-mediated electron transfer to the triosmium center takes place in **6** and **7**, but three successive C_{60}-localized reductions occur in **9**.

Introduction

Exohedral metallofullerenes have recently attracted much attention[1] concerning the effect of metal coordination on the chemical and physical properties of C_{60}. In particular, understanding of the metal substituent effect on the redox properties of C_{60} is crucial for the development of specific electronic and optical applications in materials science.[2] The electrochemical properties of the metallofullerenes have been scarcely reported, and detailed studies were precluded due to their electrochemical instabilities upon reductions.[3]

In previous work, we have reported synthesis and characterization of η^2-C_{60} and μ_3-η^2,η^2,η^2-C_{60} triosmium cluster complexes, $Os_3(CO)_{11-n}L_n(\eta^2$-$C_{60})$ ($n = 0$ (**1**); $n = 1$, L = MeCN (**2**) or PPh_3 (**3**); $n = 2$, L = PPh_3 (**4**) or PMe_3 (**5**)), $Os_3(CO)_9(\mu_3$-η^2,η^2,η^2-$C_{60})$ (**6**), and $Os_3(CO)_8(PMe_3)(\mu_3$-η^2,η^2,η^2-$C_{60})$ (**7**).[4,5] These metal cluster bound C_{60} complexes have been investigated with the expectation of seeing new bonding modes, physical properties, fluxionality, or reactivities by cooperative interactions of metal centers. As expected, we have observed a new bonding mode of a cluster face capping μ_3-η^2,η^2,η^2-C_{60} ligand in **6** and **7** and interesting fluxional processes of restricted equilibration of in-plane equatorial C_{60} and carbonyl ligands via a triply bridged intermediate in the major isomer of **2** and **5**.[5] Furthermore, electrochemical studies of **1**, **3**, and **4** have revealed the first example of novel C_{60}-mediated electron transfer to the metal center.[6] However, the first structural characterization of the arene-like μ_3-η^2,η^2,η^2-C_{60} ligand has appeared for the ruthenium analogue of **6** during our investigation.[7] As an extension of our work on this new μ_3-η^2,η^2,η^2-C_{60} ligand, we have been studying reactivities and electrochemical properties of μ_3-η^2,η^2,η^2-C_{60} triosmium complexes. Herein we report the synthesis and characterization of **6**, $Os_3(CO)_8(PPh_3)(\mu_3$-η^2,η^2,η^2-$C_{60})$ (**8**), and $Os_3(CO)_7(PMe_3)_2(\mu_3$-$\eta^2,\eta^2,\eta^2$-$C_{60})$ (**9**) and electrochemical studies of **6**, **7**, and **9**, together with the crystal structure of **8**.

Results and Discussion

Synthesis and Characterization of 6−9. We have previously reported the synthesis and characterization of $Os_3(CO)_9(\mu_3$-η^2,η^2,η^2-$C_{60})$ (**6**).[5] Its ^{13}C NMR spectrum of the carbonyl region (188−298 K) showed a single resonance at δ 176.1 for the nine carbonyls, which implies the presence of a fast localized 3-fold rotation

---

* To whom correspondence should be addressed. E-mail: jtpark@sorak.kaist.ac.kr. Fax: +82-42-869-2810.

[†] Korea Advanced Institute of Science and Technology.

[‡] Yonsei University.

(1) (a) Stephens, A.; Green, M. L. H. *Adv. Inorg. Chem.* **1997**, *44*, 1. (b) Sliwa, W. *Transition Met. Chem.* **1996**, *21*, 583. (c) Bowser, J. R. *Adv. Organomet. Chem.* **1994**, *36*, 57. (d) Fagan, P. J.; Calabrese, J. C.; Malone, B. *Acc. Chem. Res.* **1992**, *25*, 134.

(2) Prato, M. *J. Mater. Chem.* **1997**, *7*, 1097.

(3) (a) Lerke, S. A.; Parkinson, B. A.; Evans, D. H.; Fagan, P. J. *J. Am. Chem. Soc.* **1992**, *114*, 7807. (b) Koefod, R. S.; Xu, C.; Lu, W.; Shapley, J. R.; Hill, M. G.; Mann, K. R. *J. Phys. Chem.* **1992**, *96*, 2928. (c) Chernega, A. N.; Green, M. L. H.; Haggitt, J.; Stephens, H. H. *J. Chem. Soc., Dalton Trans.* **1998**, 755.

(4) Park, J. T.; Cho, J.-J.; Song, H. *J. Chem. Soc., Chem. Commun.* **1995**, 15.

(5) Park, J. T.; Song, H.; Cho, J.-J.; Chung, M.-K.; Lee, J.-H.; Suh, I.-H. *Organometallics* **1998**, *17*, 227.

(6) Park, J. T.; Cho, J.-J.; Song, H.; Jun, C.-S.; Son, Y.; Kwak, J. *Inorg. Chem.* **1997**, *36*, 2698.

(7) Hsu, H.-F.; Shapley, J. R. *J. Am. Chem. Soc.* **1996**, *118*, 9192.

S0276-7333(98)00361-6 CCC: $15.00

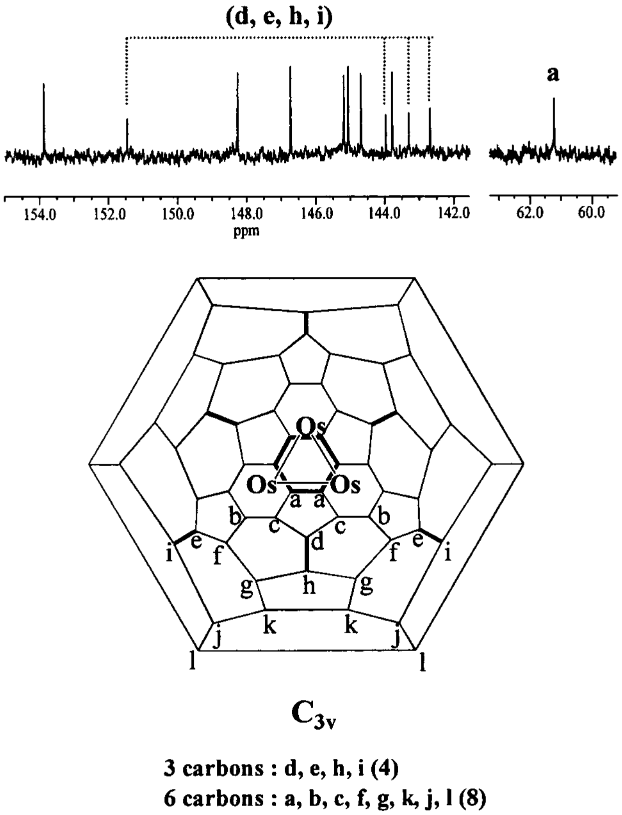

Figure 1. ^{13}C NMR spectrum (C_{60} region) of **6** in 1,2-dichlorobenzene relative to the external standard dichloromethane-d_2.

of three carbonyl groups on each atom. The ^{13}C NMR spectrum of the C_{60} region (Figure 1) is now obtained and reveals 12 resonances, at δ 153.8, 151.4, 148.2, 146.7, 145.1, 145.0, 144.7, 143.9, 143.7, 143.3, 142.7, and 61.2. The four resonances at 151.4, 143.9, 143.3, and 142.7 (dotted line) appear with about half of the intensity of the other seven resonances except the resonance at δ 61.2. This observation indicates the idealized C_{3v} symmetry of **6** in solution, which contains 12 types of carbon atoms of the C_{60} moiety, i.e., three carbon atoms of each d, e, h, and i type (bold lines) and six carbon atoms of each a, b, c, f, g, k, j, and l type, as shown in Figure 1. The six carbon atoms (a, bold lines) coordinated to the osmium metal center appear at δ 61.2 as a singlet with a lower intensity.

A triphenylphosphine-substituted complex, $Os_3(CO)_8(PPh_3)(\mu_3\text{-}\eta^2,\eta^2,\eta^2\text{-}C_{60})$ (**8**), has been prepared by initial decarbonylation of **6** with 1 equiv of Me_3NO/MeCN at 0 °C and subsequent thermolysis in chlorobenzene at 100 °C in the presence of triphenylphosphine in 50% yield. Decarbonylation of **6** with 2 equiv of Me_3NO/MeCN at 0 °C followed by treatment with PMe_3 at room temperature produces $Os_3(CO)_7(PMe_3)_2(\mu_3\text{-}\eta^2,\eta^2,\eta^2\text{-}C_{60})$ (**9**) in 49% yield. Attempted synthesis of $Os_3(CO)_7(PPh_3)_2(\mu_3\text{-}\eta^2,\eta^2,\eta^2\text{-}C_{60})$ under similar conditions resulted in a lower (ca. 20%) yield. Complexes **8** and **9** are soluble in common solvents such as dichloromethane, toluene, carbon disulfide, and chlorinated benzene to form brown (**8**) and grayish green (**9**) solutions. Formulations of **8** and **9** are established by elemental analyses and by positive ion FAB mass spectrometry. The molecular ion (M^+) isotope multiplet in the mass spectra of **8** and **9** matches perfectly the calculated pattern: the highest peaks in the M^+ multiplet (m/z, found, calcd) are (1778, 1778) for **8** and (1640, 1640) for **9**. The carbonyl region IR spectrum of **8** is similar in pattern to that reported for **7**,[5] but slightly shifted to lower energies by ca. 1−6 cm^{-1} relative to **7**, reflecting a poorer donor property of PPh_3 than PMe_3. The carbonyl region IR bands of **9** appear in the lower energy region by ca. 24 cm^{-1} compared to those of **8**. The ^{13}C NMR spectrum (CO region) of ^{13}CO-enriched **8** at 298 K shows two resonances at δ 184.8 (d, $^2J_{PC} = 5.7$ Hz) and 177.6 in a 1:3 ratio, whose general features are very similar to those of **7** (δ 185.4 (d, $^2J_{PC} = 5.9$ Hz, 2CO) and 178.5 (s, 6CO))[5] and the arene analogue $Os_3(CO)_8(PPh_3)(\mu_3\text{-}\eta^2,\eta^2,\eta^2\text{-}C_6H_6)$ (δ 183.96 (d, $^2J_{PC} = 8.0$ Hz, 2CO) and 177.39 (s, 6CO)).[8] The resonances at δ 184.8 with a P−C coupling and at δ 177.6 can be obviously assigned to the two carbonyl ligands on the osmium atom coordinated with PPh_3 and the six carbonyl groups on the other two osmium atoms, respectively. The ^{13}C NMR spectrum of ^{13}CO-enriched **9** reveals a broad resonance at δ 187.8 and a sharp resonance at 180.0 in a ratio of 4:3, which can be similarly assigned to the carbonyls on the phosphine-substituted osmium atoms and those in the unique $Os(CO)_3$ moiety, respectively. In all of these complexes, a fast localized 3-fold rotation of ligands appears to occur on each osmium center. The phosphine-substituted osmium center, however, may undergo a restricted 3-fold rotation proposed by Pomeroy and co-workers,[9] without requiring the bulky phosphine ligand to enter an axial site. The localized 3-fold rotation of ligands seems to be a general fluxional process in the $\mu_3\text{-}\eta^2,\eta^2,\eta^2\text{-}C_{60}$ triosmium carbonyl complexes. Complex **7** is much more soluble in dichlorobenzene than **8**, and thus the ^{13}C NMR spectrum of the C_{60} region has been obtained for **7**, as shown in Figure 2. The C_s symmetric nature of **7** in solution reveals three sp^3 carbon resonances (δ 57.2, 57.1, and 56.7) and 29 resonances comprising 25 and 4 (d, e, h, i denoted as ●) lines in an intensity ratio of 2:1 (see Scheme 1).

The ^{13}C NMR resonances of the C_{60} moiety for metallofullerenes have been reported for $Rh(NO)(PPh_3)_2(\eta^2\text{-}C_{60})$ (C_s symmetry, 31 sp^2 and 1 sp^3 resonances),[10] $Fe(CO)_4(\eta^2\text{-}C_{60})$ (C_{2v}, 16 sp^2 and 1 sp^3),[11] $Os_3(CO)_9(PMe_3)_2(\eta^2\text{-}C_{60})$ (C_{2v}, 16 sp^2 and 1 sp^3),[5] and $Re_2(PMe_3)_4H_8(\mu\text{-}\eta^2,\eta^2\text{-}C_{60})$ (C_s, 30 sp^2 and 2 sp^3).[3c] The chemical shifts of the C_{60} sp^2 and sp^3 carbon atoms are typically in the regions of δ 175−135 and 85−50, respectively. In these $\eta^2\text{-}C_{60}$ complexes, the sp^2 carbon atoms adjacent to the sp^3 ones (referred to as the C2 atoms) generally resonate at uniquely low fields above ca. 155 ppm, whereas those adjacent to the C2 atoms typically appear in the high-field region below ca. 140 ppm.[1a] If this generality were to hold for the $\mu_3\text{-}\eta^2,\eta^2,\eta^2\text{-}C_{60}$ moiety in **6**, the lowest and the highest field resonances at δ 153.8 and 142.7 can be assigned to the c and d type carbons, respectively.

Electrochemical Studies of 6, 7, and 9. Electrochemical properties of $\mu_3\text{-}\eta^2,\eta^2,\eta^2\text{-}C_{60}$ complexes, **6**, **7**,

---

(8) Gallop, M. A.; Gomez-Sal, M. P.; Housecroft, C. E.; Johnson, B. F. G.; Lewis, J.; Owen, S. M.; Raithby, P. R.; Wright, A. H. *J. Am. Chem. Soc.* **1992**, *114*, 2502.

(9) Alex, R. F.; Pomeroy, R. K. *Organometallics* **1987**, *6*, 2437.

(10) Green, M. L. H.; Stephens, A. H. H. *J. Chem. Soc., Chem. Commun.* **1997**, 793.

(11) Douthwaite, R. E.; Green, M. L. H.; Stephens, A. H. H.; Turner, J. F. C. *J. Chem. Soc., Chem. Commun.* **1993**, 1522.

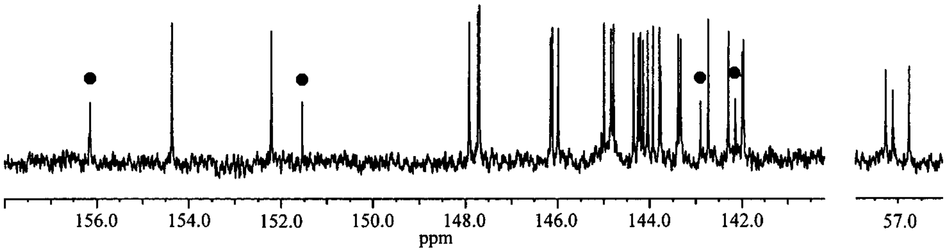

Figure 2. ^{13}C NMR spectrum (C_{60} region) of **7** in 1,2-dichlorobenzene relative to the external standard dichloromethane-d_2. Resonances due to d, e, h, and i carbons are labeled as (●).

Scheme 1

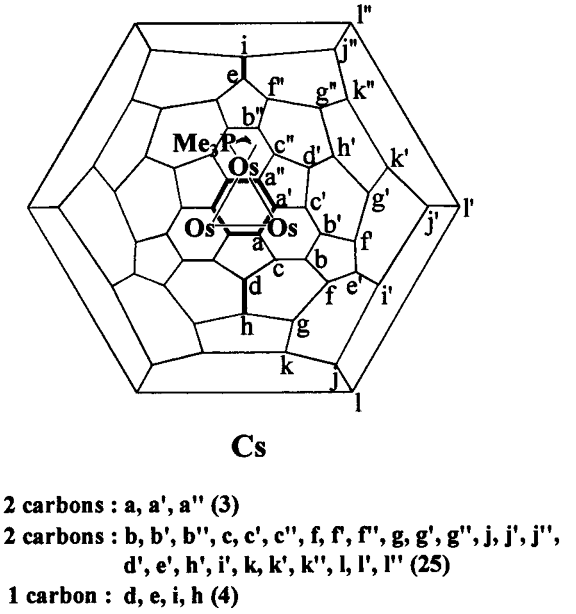

and **9**, have been examined by cyclic voltammetry in 1,2-dichlorobenzene (DCB) solutions with tetrabuthylammonium perchlorate as the supporting electrolyte. Cyclic voltammograms (CV) of **6**, **7**, and **9** are shown in Figure 3. Half-wave potentials ($E_{1/2}$) of **6**, **7**, **9**, free C_{60}, known η^2-C_{60} triosmium complexes (**1** and **4**), and two organofullerenes (**10** and **11**)[12] are summarized in Table 1. The general features of CV curves recorded for **6** and **7** reveal four reversible redox couples for **6** and three redox couples for **7**. The third redox wave of **7** corresponds to a two-electron process, while it could be resolved into two one-electron redox couples at half-wave potentials of −1.93 and −1.95 V by simulation as indicated in Table 1. The CV of **9** shows three reversible one-electron redox processes: the fourth wave is not seen due to the solvent cutoff. The number of electrons involved in each redox wave was confirmed by chronoamperometry (see the Experimental Section). Each redox couple of **7** and **9** is shifted to more negative potential (ca. 75 mV/PMe_3) compared to that of **6** due to the electron-donating nature of the phosphine ligand, as was previously observed in η^2-C_{60} triosmium complexes.

The first reduction waves of **6** and **7** are shifted to more positive potential by ca. 100 and 20 mV, respectively, in comparison with that of free C_{60}. The second reduction wave of **6** and **7** also shows an anodic shift of 130 mV for **6** and 40 mV for **7**. Transition metal C_{60} derivatives that undergo reduction more easily than unsubstituted C_{60} are not precedented.[3] Such an anodic shift of the first reduction potential, however, was observed for organofullerenes such as $C_{60}O$[13] and **11**[12] (vide infra) and is known to correlate well with the LUMO energy levels. The third reduction of **6** occurs at a potential of −1.61 V, with a significant positive shift (290 mV) relative to that of free C_{60} at −1.90 V. This unusually large positive shift suggests that the two electrons accepted through the C_{60} ligand in $\mathbf{6}^{2-}$ are delocalized to the triosmium center with its strong π-acid carbonyl ligands, as was previously proposed for $\mathbf{4}^{2-}$.[6] Dianionic species $\mathbf{6}^{2-}$ with electron delocalization to the osmium center, therefore, undergoes easier reduction via the C_{60} ligand than free $C_{60}{}^{2-}$ to afford $\mathbf{6}^{3-}$. It should be mentioned that the direct metal center reductions (two-electron process) of $Os_3(CO)_{12}$, $Os_3(CO)_{11}(PMe_3)$, and $Os_3(CO)_{10}(PMe_3)_2$ have been observed at far more negative potentials of −2.05, −2.22, and −2.53 V, respectively, under similar conditions. The fourth reduction potential (−1.74 V) of **6** is very close

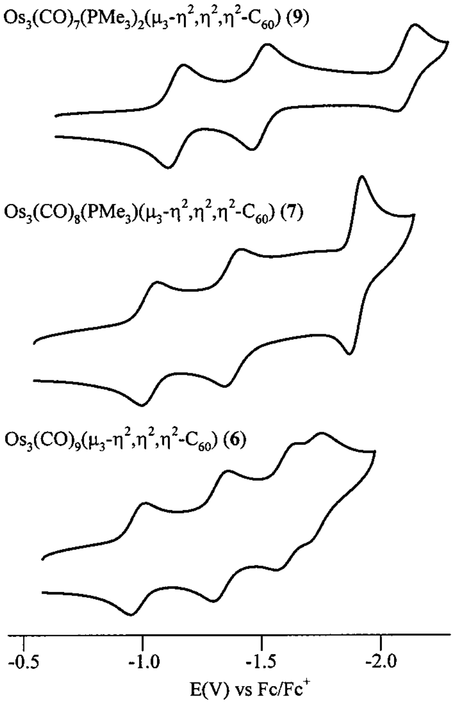

Figure 3. Cyclic voltammograms of **6**, **7**, and **9** in dry deoxygenated 1,2-dichlorobenzene (0.1 M $[(n\text{-}Bu)_4N]ClO_4$). Scan rate = 50 mV/s.

---

[12] Knight, B.; Martin, N.; Ohno, T.; Orti, E.; Rovita, C.; Veciana, J.; Vidal-Gancedo, J.; Viruela, P.; Viruela, R.; Wudl, F. *J. Am. Chem. Soc.* **1997**, *119*, 9871.

[13] Suzuki, T.; Maruyama, Y.; Akasaka, T.; Ando, W.; Kobayashi, K.; Nagase, S. *J. Am. Chem. Soc.* **1994**, *116*, 1359.

Table 1. Half-Wave Potentials ($E_{1/2}$ vs E°_{Fc/Fc^+}) of Free C_{60}, C_{60}−Triosmium Complexes, and Organofullerenes

compound		$E_{1/2}^{0/-1}$		$E_{1/2}^{-1/-2}$		$E_{1/2}^{-2/-3}$		$E_{1/2}^{-3/-4}$	solvent	ref
C_{60}		-1.05	0.36	-1.41	0.46	-1.87			DM/Tol	6
$Os_3(CO)_{11}(\eta^2\text{-}C_{60})$	**1**	-1.08	0.23[b]	-1.31	0.30	-1.61[a]			DM/Tol	6
$Os_3(CO)_9(PPh_3)_2(\eta^2\text{-}C_{60})$	**4**	-1.19	0.34	-1.53	0.23[b]	-1.76[a]			DM/Tol	6
C_{60}		-1.08	0.38	-1.46	0.44	-1.90	0.48	-2.38	DCB	d
$Os_3(CO)_9(\mu_3\text{-}\eta^2,\eta^2,\eta^2\text{-}C_{60})$	**6**	-0.98	0.35	-1.33	0.28[b]	-1.61	0.13[b]	-1.74	DCB	d
$Os_3(CO)_8(PMe_3)(\mu_3\text{-}\eta^2,\eta^2,\eta^2\text{-}C_{60})$	**7**	-1.06	0.36	-1.42	0.51	-1.93	0.02[b]	-1.95	DCB	d
$Os_3(CO)_7(PMe_3)_2(\mu_3\text{-}\eta^2,\eta^2,\eta^2\text{-}C_{60})$	**9**	-1.13	0.35	-1.48	0.61	-2.09			DCB	d
C_{60}		-1.123[a]	0.33	-1.455[a]	0.44	-1.913[a]	0.47	-2.383[a]	DCB	12
spiro[3,5-dimethyl-2,5-cyclohexadienone-4-61'-methanofullerene]	**10**	-1.042[a]	0.16[c]	-1.197[a]	0.41	-1.602[a]			DCB	12
spiro[10-anthrone-9,61'-methanofullerene]	**11**	-1.215[a]	0.31[c]	-1.525[a]	0.15	-1.670[a]			DCB	12

[a] The cathodic peak potential. [b] Difference in reduction potentials of each species in which electron delocalization from C_{60} to triosmium has occurred. [c] Addend reductions. [d] This work.

to the third reduction potential (−1.61 V) and even more positive than the third reduction of C_{60} (−1.90 V), which implies that further electron delocalization from C_{60} to the metal center occurred in **6**$^{3-}$ as well. Comparable first through third reduction potentials of **7** to those of free C_{60} indicate that three successive C_{60}-localized reductions occur to produce **7**$^{1-}$, **7**$^{2-}$, and **7**$^{3-}$. Similarly, three redox waves of **9** appear at more negative potentials than those of free C_{60} by ca. 50−190 mV. The third and fourth reductions of **7**, however, take place essentially at the same potential. This observation further supports the conclusion that the electron density in **7**$^{3-}$ is also significantly delocalized to the triosmium center, resulting in a large positive shift of the fourth reduction potential of **7**.

Recently Wudl and co-workers[12] reported electrochemical studies and quantum-chemical calculation of spiroannelated methanofullerenes, **10** and **11** (see Table 1), to understand the electronic effect of organic addends on the molecular orbitals and redox properties of C_{60}. The anodic shift (81 mV) of the first reduction potential of **10** with respect to C_{60} has been explained by the inductive effect of the electronegative cyclohexadienone addend on the stabilization of the LUMO localized on the C_{60} cage. The dianionic species of **10** and **11** were proposed to have an open structure where one of the cyclopropane−C_{60} bonds is broken and each electron is localized on both C_{60} and the addend (cyclohexadienone for **10** and quinone for **11**). **10**$^{2-}$ and **11**$^{2-}$ were reported to undergo reductions through the C_{60} ligand at potentials −1.602 and −1.670 V, which are very similar to the reduction potentials of −1.61 V for **1**$^{2-}$, −1.76 V for **4**$^{2-}$, and −1.61 V for **6**$^{2-}$. Similar third reduction potentials among dianionic species **1**$^{2-}$, **4**$^{2-}$, **6**$^{2-}$, **10**$^{2-}$, and **11**$^{2-}$ imply that electrons in **1**$^{2-}$, **4**$^{2-}$, and **6**$^{2-}$ are appreciably delocalized to the triosmium addend in analogy with **10**$^{2-}$ and **11**$^{2-}$ with a negative charge on the addend. IR spectroelectrochemical studies of **6** and **7** have been attempted to obtain definitive evidence for the C_{60}-mediated electron transfer to the triosmium center. The IR spectra obtained for each anionic species were very poorly defined, presumably because of incomplete reductions of each species during the spectroelectrochemical experiment.

Electrochemical studies of transition metal C_{60} complexes have been reported for metallofullerenes such as $[(Et_3P)_2M]_n(\eta^2\text{-}C_{60})$ (M = Ni, Pd, Pt; n = 1−4),[3a] $(\eta^5\text{-}C_9H_7)Ir(CO)(\eta^2\text{-}C_{60})$,[3b] and $Co(NO)(PPh_3)_2(\eta^2\text{-}C_{60})$,[3c] which revealed C_{60}-localized sequential reductions. These C_{60}-localized reductions are well documented in both metallofullerenes[3] and organofullerenes,[12,13] whose redox potentials are slightly modified in comparison with free C_{60} by the metal-to-C_{60} π-back-donation or the inductive effect of the attached organic moiety. Either metal complexation or electron-donating organic addend is known to raise the energy of the C_{60}-localized LUMO and thus decreases the electron affinity of C_{60}. Cyclic voltammetric and IR spectroelectrochemical studies of η^2-C_{60} triosmium complexes **1**, **3**, and **4**, however, showed a C_{60}-mediated electron transfer to the triosmium metal center (see $E_{1/2}^{-1/-2}$ for **1** and $E_{1/2}^{-2/-3}$ for **4** in Table 1).[6] This unusual electronic communication between C_{60} and the metal center has also been observed in μ_3-η^2,η^2,η^2-C_{60} triosmium complexes **6** and **7**. All the known η^2-C_{60} transition metal complexes undergo metal dissociation in the reduced anions,[3,6] because the additional electrons are accommodated in a LUMO that is derived from both the 29 double bonds of C_{60} and a component of the metal−C_{60} antibonding orbital.[3c] The μ_3-η^2,η^2,η^2-C_{60} triosmium complexes **6**, **7**, and **9** with three metal−C_{60} π-bonds, however, have shown a remarkable electrochemical stability and a reversible behavior for redox processes with as many as four redox couples in the DCB potential window.

Crystal Structure of 8·1.5CS$_2$. The overall molecular geometry and the atomic labeling scheme of **8** are illustrated in Figure 4. Interatomic distances and angles are listed in Tables 2 and 3, respectively.

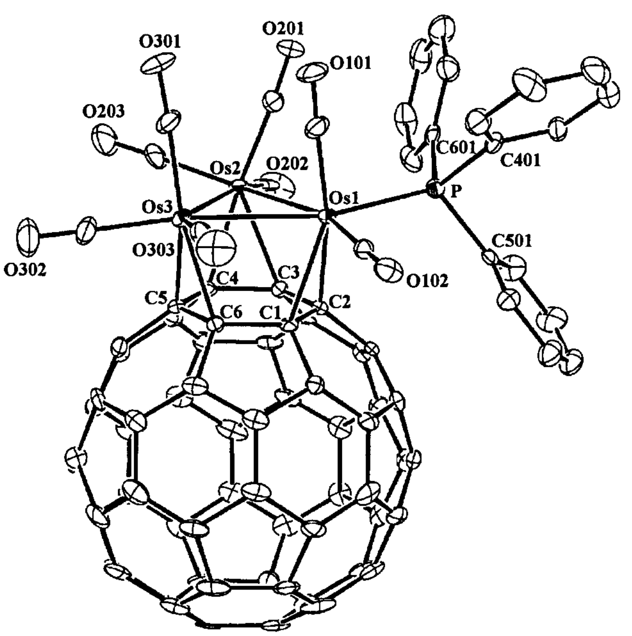

Figure 4. Molecular geometry and atomic-labeling scheme for **8**.

Table 2. Selected Interatomic Distances (Å) and Esd's for 8·1.5CS$_2$

(A) Metal−Metal Distances			
Os(1)−Os(2)	2.956(1)	Os(1)−Os(3)	2.888(1)
Os(2)−Os(3)	2.907(1)		
(B) Metal−Carbon (Carbonyl) Distances			
Os(1)−C(101)	1.89(2)	Os(1)−C(102)	1.84(2)
Os(2)−C(201)	1.92(2)	Os(2)−C(202)	1.92(2)
Os(2)−C(203)	1.87(2)	Os(3)−C(301)	1.91(2)
Os(3)−C(302)	1.88(2)	Os(3)−C(303)	1.90(2)
(C) Metal−Phosphorus Distances			
Os(1)−P	2.370(4)		
(D) Carbon−Oxygen (Carbonyl) Distances			
C(101)−O(101)	1.15(2)	C(102)−O(102)	1.16(2)
C(201)−O(201)	1.13(2)	C(202)−O(202)	1.12(2)
C(203)−O(203)	1.15(2)	C(301)−O(301)	1.15(2)
C(302)−O(302)	1.15(2)	C(303)−O(303)	1.15(2)
(E) Metal−Carbon (C_{60}) Distances			
Os(1)−C(1)	2.32(1)	Os(1)−C(2)	2.30(1)
Os(2)−C(3)	2.31(1)	Os(2)−C(4)	2.22(1)
Os(3)−C(5)	2.31(1)	Os(3)−C(6)	2.25(1)
(F) Distances within the C_{60} Ligand			
C(1)−C(2)	1.43(2)	C(2)−C(3)	1.45(2)
C(3)−C(4)	1.48(2)	C(4)−C(5)	1.46(2)
C(5)−C(6)	1.45(2)	C(1)−C(6)	1.46(2)

The molecular structure of **8** is derived from that of $Os_3(CO)_{11}(PPh_3)$ by replacing three axial carbonyl groups on three osmium atoms with the C_{60} ligand. A six-membered carbon ring (C_6 ring) of the C_{60} ligand positions centrally over the Os_3 framework, as was shown in $Ru_3(CO)_9(\mu_3$-η^2,η^2,η^2-$C_{60})$ (**12**).[7] The C_6 ring is essentially parallel with the Os_3 plane with a dihedral angle of 1.2° [cf. 0.9° for **12**[7] and 1.2° for $Os_3(CO)_8(PPh_3)(\mu_3$-η^2,η^2,η^2-$C_6H_6)$ (**13**)[8]]. The two $Os(CO)_3$ and one $Os(CO)_2(PPh_3)$ units are slightly twisted, all in the same direction, so that the three axial carbonyls are disposed in a propeller-like configuration. Each pair of equatorial ligands is placed one above and one below the Os_3 plane. The bulky phosphine ligand occupies an equatorial position and is disposed away from the C_{60} ligand, presumably due to its unfavorable steric interaction with the C_{60} ligand.

Table 3. Selected Interatomic Angles (deg) and Esd's for 8·1.5CS$_2$

(A) Intermetallic Angles			
Os(2)−Os(1)−Os(3)	59.64(2)	Os(1)−Os(2)−Os(3)	59.01(2)
(B) M−M−CO and M−M−P Angles			
Os(2)−Os(1)−C(101)	92.7(5)	Os(3)−Os(1)−C(101)	81.6(5)
Os(2)−Os(1)−C(102)	163.2(4)	Os(3)−Os(1)−C(102)	105.0(4)
Os(2)−Os(1)−P	105.1(1)	Os(3)−Os(1)−P	162.4(1)
Os(1)−Os(2)−C(201)	80.6(5)	Os(3)−Os(2)−C(201)	101.0(5)
Os(1)−Os(2)−C(202)	125.4(5)	Os(3)−Os(2)−C(202)	167.4(4)
Os(1)−Os(2)−C(203)	139.1(7)	Os(3)−Os(2)−C(203)	83.2(7)
Os(1)−Os(3)−C(301)	96.9(5)	Os(2)−Os(3)−C(301)	81.8(6)
Os(1)−Os(3)−C(302)	173.1(5)	Os(2)−Os(3)−C(302)	119.9(6)
Os(1)−Os(3)−C(303)	82.8(5)	Os(2)−Os(3)−C(303)	143.8(5)
(C) Os−C−O, C−Os−C, and C−Os−P Angles			
Os(1)−C(101)−O(101)	178(1)	Os(1)−C(102)−O(102)	179(1)
Os(2)−C(201)−O(201)	174(2)	Os(2)−C(202)−O(202)	175(1)
Os(2)−C(203)−O(203)	177(2)	Os(3)−C(301)−O(301)	177(2)
Os(3)−C(302)−O(302)	179(2)	Os(3)−C(303)−O(303)	176(2)
C(101)−Os(1)−C(102)	91.4(6)	C(101)−Os(1)−P	90.9(5)
C(102)−Os(1)−P	91.1(4)	C(201)−Os(2)−C(202)	91.5(7)
C(201)−Os(2)−C(203)	93.2(7)	C(202)−Os(2)−C(203)	94.9(8)
C(301)−Os(3)−C(302)	90.0(7)	C(301)−Os(3)−C(303)	99.4(8)
C(302)−Os(3)−C(303)	96.3(7)		
(D) Angles Involving Metal-Coordinated Carbon in C_{60}			
C(2)−C(1)−C(6)	121(1)	C(1)−C(2)−C(3)	119(1)
C(2)−C(3)−C(4)	121(1)	C(3)−C(4)−C(5)	118(1)
C(4)−C(5)−C(6)	121(1)	C(1)−C(6)−C(5)	120(1)

The Os(1)−Os(2) distance (2.956(1) Å) is notably longer than the other two Os−Os distances (2.888(1) and 2.907(1) Å), which is apparently ascribed to the repulsion between the phenyl groups of the phosphine ligand and the carbonyl ligands on Os(2) atom. The average Os−Os distance for **8** (2.917(1) Å) is longer than that for $Os_3(CO)_{12}$ (2.877(3) Å).[14] The Os−C(C_{60}) bonds alternate in length, with the average long distance of 2.31(1) Å and the average short distance of 2.26(3) Å, which leads to the slight twist of the C_6 ring of the C_{60} ligand over the triangular Os_3 framework. However, the carbon−carbon bonds of the C_6 ring do not appear to alternate in length, ranging from 1.43(2) Å to 1.48(2) Å (av 1.46(2) Å). The C_6 ring is pulled away from the C_{60} surface, consistent with the change in the hybridization to sp^3. The average angle between the metal-coordinated C−C bond vector at the 6,6 ring junction and the plane defined by one of the two carbon atoms and its two neighboring sp^2 and sp^3 carbon atoms is 35(1)°, which is larger than the free C_{60} value of 31° [15] [cf. 40(2)° for **1**[5] and 41(2)° for $Pt(PPh_3)_2(\eta^2$-$C_{60})$[15]]. A small degree of bond alternation, however, has been observed for the benzene analogue **13** (av 1.43(2) and av 1.40(2) Å)[8] and for the triruthenium complex **12** (av 1.466(15) and 1.427(19) Å).[7]

All other features of the molecular geometry are within the expected range. The average C−C bond length at the junctions of the 5,6 ring is 1.45(2) Å, and that at the junctions of the 6,6 ring is 1.39(2) Å. The Os−CO distances range from 1.84(2) to 1.92(2) Å, C−O bond lengths range from 1.12(2) through 1.16(2) Å, and ∠Os−C−O angles are in the range of 174(2)−179(2)°. The CS_2 solvate molecules do not enter into any significant interactions with molecule **8**.

---

(14) Churchill, M. R.; DeBore, B. G. *Inorg. Chem.* **1977**, *16*, 878.

(15) Fagan, P. J.; Calabrese, J. C.; Malone, B. *Science* **1991**, *252*, 1160.

Experimental Section

General Comments. All reactions were carried out under a nitrogen atmosphere with use of standard Schlenk techniques. Solvents were dried appropriately before use. C_{60} (99.5%, Southern Chemical Group, LLC) was used without further purification. Anhydrous trimethylamine *N*-oxide (mp 225−230 °C) was obtained from $Me_3NO{\cdot}2H_2O$ (98%, Aldrich Chemical Ltd.) by sublimation (three times) at 90−100 °C under vacuum. $Os_3(CO)_{11}(NCMe)$,[16] $Os_3(CO)_9(\mu_3\text{-}\eta^2,\eta^2,\eta^2\text{-}C_{60})$ (**6**),[5] and $Os_3(CO)_8(PMe_3)(\mu_3\text{-}\eta^2,\eta^2,\eta^2\text{-}C_{60})$ (**7**)[5] were prepared by the literature methods. Carbon-13 (*C) CO enriched complexes were prepared by using $Os_3(^*CO)_{12}$ (ca. 35% enrichment).[17] Preparative thin layer plates were prepared with silica gel GF_{254} (type 60, E. Merck).

Infrared spectra were obtained on a Bruker EQUINOX-55 FT-IR spectrophotometer. ^1H (300 MHz), ^{13}C (75 MHz), and ^{31}P (122 MHz) NMR spectra were recorded on a Bruker AM-300 spectrometer. Positive ion FAB mass spectra (FAB$^+$) were obtained by the staff of the Korea Basic Science Center. All *m*/*z* values are referenced to ^{192}Os. Elemental analyses were provided by the staff of the Agency for Defense Development.

^{13}C NMR Data (C_{60} Region) of 6 and 7. Compound **6**: $^{13}C\{^1H\}$ NMR ($C_6H_4Cl_2$/ext. CD_2Cl_2, 298 K) δ 153.8 (6C), 151.4 (3C), 148.2 (6C), 146.7 (6C), 145.1 (6C), 145.0 (6C), 144.7 (6C), 143.9 (3C), 143.7 (6C), 143.3 (3C), 142.7 (3C), 61.2 (6C, C_{60} sp^3 carbon). Compound **7**: $^{13}C\{^1H\}$ NMR ($C_6H_4Cl_2$/ext. CD_2Cl_2, 298 K) δ 156.1 (1C), 154.3 (2C), 152.2 (2C), 151.5(1C), 147.9 (2C), 147.7 (2C), 147.6 (2C), 146.1 (2C), 146.1 (2C), 146.0 (2C), 145.0 (2C), 144.8 (2C), 144.8 (2C), 144.3 (2C), 144.2 (2C), 144.2 (2C), 144.1 (2C), 144.0 (2C), 143.9 (2C), 143.8 (2C), 143.7 (2C), 143.4 (2C), 143.3 (2C), 142.9 (1C), 142.7 (2C), 142.3 (2C), 142.1 (1C), 142.0 (2C), 142.0 (2C), 57.2 (2C, C_{60} sp^3 carbon), 57.1 (2C, C_{60} sp^3 carbon), 56.7 (2C, C_{60} sp^3 carbon).

Preparation of $Os_3(CO)_8(PPh_3)(\mu_3\text{-}\eta^2,\eta^2,\eta^2\text{-}C_{60})$ (8). Compound **6** (20.0 mg, 0.0130 mmol) and an excess amount (10.2 mg, 0.0389 mmol) of PPh_3 were dissolved in chlorobenzene (20 mL). The solution was cooled to 0 °C, and an acetonitrile solution (3 mL) of anhydrous Me_3NO (1.1 mg, 0.015 mmol) was added dropwise. The reaction mixture was allowed to warm to room temperature for 30 min. After evaporation of the solvent in vacuo, the residue was dissolved in chlorobenzene (20 mL). The reaction mixture was stirred at 100 °C for 1 h. The solvent was evaporated, and the residue was purified by preparative TLC (CS_2) to afford compound **8** (11.5 mg, 0.0065 mmol, 50%, $R_f = 0.4$) as a brown solid: IR (CS_2) ν(CO) 2064 (vs), 2033 (s), 2013 (m), 1999 (m), 1983 (m), 1952(w) cm^{-1}; ^1H NMR ($CDCl_3$, 298 K) δ 7.35 (m, 18H); $^{31}P\{^1H\}$ NMR ($CDCl_3$, 298 K) δ 9.64 (s); $^{13}C\{^1H\}$ NMR ($C_6H_4Cl_2$/ext. CD_2Cl_2, 298 K) δ 184.8 (d, $^2J_{PC} = 5.7$ Hz, 2CO), 177.6 (s, 6CO); MS (FAB$^+$) *m*/*z* 1778 (M$^+$). Anal. Calcd for $C_{89}H_{15}O_8PS_6Os_3$ ($\mathbf{8}{\cdot}3CS_2$): C, 53.3; H, 0.75; S, 9.59. Found: C, 53.6; H, 0.40; S, 10.4.

Preparation of $Os_3(CO)_7(PMe_3)_2(\mu_3\text{-}\eta^2,\eta^2,\eta^2\text{-}C_{60})$ (9). Compound **6** (30.0 mg, 0.0194 mmol) was dissolved in chlorobenzene (20 mL), and an excess amount (0.01 mL, 0.1 mmol) of PMe_3 was added. The solution was cooled to 0 °C, and an acetonitrile solution (6 mL) of anhydrous Me_3NO (2.9 mg, 0.039 mmol, 2 equiv) was added dropwise. The reaction mixture was allowed to warm to room temperature for 1 h. Evaporation of the solvent and purification by preparative TLC (CS_2) produced compound **9** (15.5 mg, 0.0095 mmol, 49%, $R_f = 0.2$) as a black solid: IR (CS_2) ν(CO) 2040 (vs), 2001 (s), 1985 (s), 1972 (m), 1957 (m), 1925(m) cm^{-1}; ^1H NMR ($CDCl_3$, 298 K) δ 1.92 (d, $^2J_{PH} = 10.1$ Hz, 18H);$^{13}C\{^1H\}$ NMR ($C_6H_4Cl_2$/ext. CD_2Cl_2, 298 K) δ 187.8 (br, 4CO), 180.0 (s, 3CO); $^{31}P\{^1H\}$ NMR ($CDCl_3$, 298 K) δ −49.6 (s); MS (FAB$^+$) *m*/*z* 1640 (M$^+$). Anal. Calcd for $C_{74}H_{18}O_7P_2S_2Os_3$ ($\mathbf{9}{\cdot}CS_2$): C, 52.3; H, 1.06; S, 3.74. Found: C, 52.6; H, 0.87; S, 3.75.

Table 4. Crystal and Structure Determination Data for $\mathbf{8}{\cdot}1.5CS_2$

formula	$C_{86}H_{15}O_8POs_3{\cdot}1.5CS_2$
fw	1891.74
system	monoclinic
space group	*C*2/*c*
a, Å	24.9899(4)
b, Å	10.0038(1)
c, Å	45.6698(5)
β, deg	90.663(1)
V, Å^3	11416.4(2)
Z	8
D_{calcd}, Mg m^{-3}	2.201
temp, K	293(2)
λ (Mo Kα), Å	0.71073
μ, mm^{-1}	6.886
transmission factors	0.49−1.00
no. of rflns measd	23468
no. of unique rflns	7926
no. of rflns ($F_o > 4\sigma(F_o)$)	6896
$R_f{}^a$	0.0630
$R_w{}^b$	0.1339

[a] $R_f = \Sigma||F_o| - |F_c||/\Sigma|F_o|$. [b] $R_w = [\Sigma\omega(|F_o| - |F_c|)^2/\Sigma\omega|F_o|^2]^{1/2}$.

Electrochemical Measurements. Cyclic voltammetry and chronoamperometry were carried out on a BAS 100B (Bioanalytical Systems, Inc.) electrochemical analyzer using the conventional three-electrode system of a platinum working electrode (1.6 mm diameter disk, Bioanalytical Systems, Inc.), a platinum counter wire electrode (5 cm length of 0.5 mm diameter wire), and a Ag/Ag$^+$ reference electrode (0.1 M $AgNO_3$/Ag in acetonitrile with a Vycor salt bridge). All measurements were performed at ambient temperature under nitrogen atmosphere in a dry deoxygenated 0.1 M 1,2-dichlorobenzene solution of $[(n\text{-}Bu)_4N]ClO_4$. The concentrations of compounds are ca. 3×10^{-4} M. All potentials are referenced to the standard ferrocene/ferrocenium (Fc/Fc$^+$) scale. The relative number of electrons involved in each reduction process was obtained from the graph of current vs (time)$^{-1/2}$ according to the Cottrell equation.[18]

X-ray Structure Determination for $\mathbf{8}{\cdot}1.5CS_2$. Crystals of **8** suitable for an X-ray analysis were grown at room temperature from a carbon disulfide solution of **8**. A dark brown crystal with approximate dimensions 0.89 × 0.09 × 0.09 mm was mounted on a glass fiber, transferred to a Siemens SMART diffractometer/CCD area detector employing a 3 kW sealed tube X-ray source operating at 2 kW, and centered in the beam.[19] Data were collected at room temperature for 12 h. Preliminary orientation matrix and cell constants were determined with a set of 20 data frames with 30 s collection per frame, followed by spot integration and least-squares refinement. A hemisphere of data was collected using 0.3° ω scans at 30 s per frame. The raw data were integrated (XY spot spread = 1.60, Z spot spread = 0.6), and the unit cell parameters were refined using SAINT.[20] Data analysis and absorption correction were performed by using Siemens XPREP.[21] The data were corrected for Lorentz and polarization effects, but no correction for crystal decay was applied. Details of the relevant crystallographic data are given in Table 4. Scattering factors and anomalous dispersion terms were taken from standard tables.

---

(16) Johnson, B. F. G.; Lewis, J.; Pippard, D. A. *J. Chem. Soc., Dalton Trans.* **1981**, 407.

(17) Clauss, A. D.; Tachikawa, M.; Shapley, J. R.; Pierpont, C. G. *Inorg. Chem.* **1981**, *20*, 1528.

(18) Bard, A. J.; Faulkner, L. R. *Electrochemical Methods*; John Wiley & Sons: New York, 1980; pp 142−146.

(19) SMART Area-Detector Software Package; Siemens Analytical Instrumentation, Inc.: Madison, WI, 1995.

(20) SAINT; SAX Area-Detector Integration Program, version 4.050; Siemens Analytical Instrumentation, Inc.: Madison, WI, 1995.

(21) XPREP: part of the SHELXTL, Crystal Structure Determination Package, version 5.04; Siemens Analytical Instrumentation, Inc.: Madison, WI, 1994.

The structure was determined by direct methods; positions for the osmium atoms were deduced from an E map. One cycle of isotropic least-squares refinement followed by an unweighted difference Fourier synthesis revealed positions for the osmium and remaining non-hydrogen atoms. Hydrogen atoms were not included in the final structure factor calculations. All non-hydrogen atoms were refined with anisotropic thermal coefficients. Successful convergence of full-matrix least-squares refinement on F^2 was indicated by the maximum shift/error for the final cycle. The final difference Fourier map had no significant features. For all computations the SHELX93 package[22] was used, and the function minimized was $\sum\omega(|F_o| - |F_c|)^2$, with $\omega = 1/[\sigma^2(F_o^2) + (0.1123P)^2]$, where $P = (F_o^2 + 2F_c^2)/3$. The number of parameters refined was 888. Final reliability factors for 7926 unique observed reflections [$F_o > 4\sigma(F_o)$] were $R_f = 0.0630$, $R_w = 0.1339$, with $(\Delta/\sigma)_{max} = 0.001$, $\Delta\rho_{max}/\Delta\rho_{min} = 2.029/-2.277$ e/Å^3 in the final $\Delta\rho$ map, and $S = 1.274$.

Acknowledgment. We are grateful to the Korea Advanced Institute of Science and Technology (KAIST) for financial support of this research. We thank Prof. J. Kwak at KAIST for help in electrochemical measurements.

Supporting Information Available: A figure of the molecular geometry with a complete atomic-labeling scheme, and tables of atomic coordinates and equivalent isotropic displacement parameters, anisotropic displacement parameters, and complete bond lengths and angles for complex **8** (13 pages). Ordering information is given on any current masthead page.

OM980361B

---

(22) Sheldrick, G. M. SHELX93, Program for Crystal Structure Refinement; University of Göettingen, Germany, 1993.